Bull. Chem. Soc. Ethiop. **2026**, 40(12), 2685-2699.
DOI: https://dx.doi.org/10.4314/bcse.v40i12.13

ISSN 1011-3924
Printed in Ethiopia
Online ISSN 1726-801X
© 2026 Chemical Society of Ethiopia and The Authors

CHEMICAL CONSTITUENTS AND BIOACTIVITIES OF *BEILSCHMIEDIA BIDOUPENSIS*

Pham Chau Anh[1], Dau Xuan Duc[1], Nguyen Dang Khoa[2,3], Nguyen Minh Chanh[2,3], Hieu Nguyen-Ngoc[4], Nguyen Thi Chung[1], Nguyen Thi Thanh Huyen[1], Phan Thi Hoai Nam[1], Hieu Tran-Trung[1*], Le Duc Giang[1*]

[1]Department of Chemistry, Vinh University, Nghean, 43100, Vietnam
[2]Institute of Applied Science and Technology, Van Lang School of Technology, Van Lang University, Ho Chi Minh City, 70000, Vietnam
[3]Faculty of Applied Technology, Van Lang School of Technology, Van Lang University, Ho Chi Minh City, 70000, Vietnam
[4]Faculty of Pharmacy, Phenikaa University, Hanoi, 10000, Vietnam

(Received June 21, 2026; Revised September 04, 2026; Accepted September 17, 2026)

ABSTRACT. For the first time, the isolation and structural elucidation of constituents of *Beilschmiedia bidoupensis* leaves, as well as their antioxidant and anti-enzymatic activities, and molecular docking study, were investigated. From the methanol extract, eight compounds were isolated and structurally elucidated, including lupeol (**1**), lupenone (**2**), betulin (**3**), 4-hydroxybenzaldehyde (**4**), β-sitosterol (**5**), quercetin (**6**), ursolic acid (**7**), and betulinic acid (**8**). Their chemical structures were elucidated by spectroscopic methods such as one- and two-dimensional nuclear magnetic resonance (1D- and 2D-NMR) spectroscopy, electrospray ionization mass spectrometry (ESI-MS), and confirmed by comparison with reference data. Among the isolates, **6** exhibited the most potent antioxidant activity in both DPPH and ABTS assays. Compound **6** also showed the lowest IC_{50} value against α-glucosidase (31.1 ± 3.14 μM), whereas ursolic acid (**7**) exhibited lower inhibitory potency. Finally, molecular docking studies were conducted to elucidate the binding interactions between the antioxidant compounds and the Keap1 protein target.

KEY WORDS: *Beilschmiedia bidoupensis*, Chemical constituent, Antioxidant, Anti-enzymatic

INTRODUCTION

Lauraceae is one of the most important families of Angiosperms and consists of 55 genera and over 2000 species [1, 2]. Among these, *Beilschmiedia* Nees is notable for being one of the largest pantropical genera that contains about 250 species distributed in Asia and Africa [2-4]. In traditional medicine, some species of the genus have been used for treating several health conditions. In Africa, the bark and leaves of some *Beilschmiedia* species are used in traditional medicine for the treatment of uterine tumors, rheumatism, and pulmonary disorders, while the fruits have been utilized as appetite stimulants and also as spices [5]. In addition, *B. anacardioides* stem bark has been employed in the Western Region of Cameroon to cure uterine tumors, rubella, female genital infections, and rheumatism [6]. In Madagascar, the fruit, bark, and leaves of *B. cryptocaryoides* have been used by the local population to treat infectious diseases and malaria [7]. Phytochemical studies have revealed highly diverse compositions within the *Beilschmiedia* species. For example, the essential oils of five *Beilschmiedia* species from Costa Rica (*B. alloiophylla*, *B. brenesii*, *B. costaricensis*, *B. tilaranensis*, and *Beilschmiedia* spp.) were analyzed by GC-MS, revealing highly varied volatile chemical profiles [8]. Studies on the isolation of the *Beilschmiedia* species have resulted in the identification of several substance groups, including flavonoids [5], lignans [9], endiandric acid derivatives [2, 10], alkaloids [11, 12], and terpenoids

*Corresponding author. E-mail: trantrunghieu94tc@gmail.com and leducgiang@gmail.com
This work is licensed under the Creative Commons Attribution 4.0 International License

[13]. Moreover, they have been associated with diverse bioactivities, such as antioxidant, anti-enzymatic, antibacterial, anti-inflammatory, and cytotoxic effects, among others [5, 7, 9-14].

Beilschmiedia bidoupensis (Figure 1), recently reported as a new species from Bidoup-Nui Ba National Park, Vietnam, is distinguished by its small, whitish-brown, hairy terminal buds, glabrous twigs, and elliptic, acuminate leaves [15]. To date, there have been no published reports on the chemical and biological data of this plant. As part of an ongoing survey of new Vietnamese medicinal plants [16-19], *B. bidoupensis* was investigated. In this paper, the isolation and the structural elucidation of eight compounds are described. Furthermore, antioxidant and anti-enzymatic activities and molecular docking studies of isolated compounds are examined. This is the first report on chemical constituents and biological activity of *B. bidoupensis*.

Figure 1. *Beilschmiedia bidoupensis* from Vietnam (photo by Cuong, T.Q.).

EXPERIMENTAL

Plant material

The leaves of *B. bidoupensis* were collected from Bidoup Nui Ba National Park, Lac Duong, Lam Dong (12°09'28.10"N 108°32'07.02" E), Vietnam, in January 2025 and identified by Assoc. Prof. Dr. Nguyen Hoang Tuan (Faculty of Pharmacognosy and Traditional Medicine, Hanoi University of Pharmacy, Vietnam). Voucher specimen (029-BB012025) was deposited at the Herbarium of the Department of Chemistry, Vinh University, Vietnam.

General experimental procedures

The ESI-MS was measured on a Shimadzu LC-MS-8045 (Shimadzu Corporation, Japan). The NMR spectra were recorded on a Bruker 600 MHz spectrometer with methanol-d_4, $CDCl_3$, and DMSO-d_6 as solvents, and the chemical shifts are expressed as δ values (ppm). Column chromatography was carried out using silica gel and reversed-phase C-18 (Merck KGaA, Darmstadt) as the stationary phase. Analytical and preparative TLCs were carried out on precoated Kieselgel 60 F254 or RP18 plates (Merck KGaA, Darmstadt). The spots were detected by spraying with 5% aqueous H_2SO_4, followed by heating with a heat gun.

Extraction and isolation

The dried leaves of *B. bidoupensis* (3.0 kg) were ground into powder and then ultrasonically extracted with methanol (15 L × 2 h × 3 times) to obtain 175 g crude extract. This extract was suspended in distilled water and sequentially partitioned with n-hexane, ethyl acetate, and n-butanol to yield the corresponding fractions: BBLH (62.5 g), BBLE (82.7 g), and BBLB (20.0 g). The fraction BBLH (50 g) was chromatographed on a silica gel column eluting with hexane/acetone (90/1–1/1, v/v) to give seven fractions (BBLH1–BBLH7). Fraction BBLH3 (5.7 g) was separated on a silica gel column eluting with hexane/EtOAc (40/1–1/1, v/v) to obtain five subfractions (BBLH3.1–BBLH3.5). The fraction BBLH3.4 (1.3 g) was further separated on a silica gel column eluting with CH_2Cl_2/acetone (15/1–1/1, v/v) to yield **2** (32.0 mg). Fraction BBLH3.5 (942 mg) was separated on a silica gel column eluting with CH_2Cl_2/acetone (12/1–1/1, v/v), then continuously purified by preparative TLC to obtain yield **4** (10.4 mg). Fraction BBLH5 (8.9 g) was subjected to a silica gel column eluting with hexane/acetone (20/1–1/1, v/v) to give four subfractions (BBLH5.1–BBLH5.4). Fraction BBLH5.2 (1.6 g) was separated on a silica gel column eluting with hexane/EtOAc (18/1–1/1, v/v) to obtain **5** (47.4 mg) and **1** (21.9 mg). Fraction BBLH5.3 (682 mg) was separated on a silica gel column eluted with CH2Cl2/acetone (14/1–1/1, v/v), then continuously purified by using preparative TLC to obtain **3** (20.3 mg).

Fraction BBLE (70 g) was chromatographed on a silica gel column eluting with CH_2Cl_2/MeOH (60/1–1/1, v/v) to yield 6 main fractions (BBLE1–BBLE6). Fraction BBLE4 (4.5 g) was separated on a silica gel column eluting with $CHCl_3$/MeOH (40/1–3/1, v/v) to obtain 8 subfractions (BBLE4.1–BBLE4.8). Fraction BBLE4.3 (1.0 g) was chromatographed on a silica gel column eluting with CH_2Cl_2/acetone (10/1–1/1, v/v) and then purified by HPLC (MeCN/H_2O, isocratic 50%–50%) to obtain **7** (12.9 mg) and **8** (11.5 mg). Fraction BBLE5 (3.1 g) was repeated on a silica gel column eluting with CH_2Cl_2/EtOAc (30/1–1/1, v/v) to obtain 3 subfractions (BBLE5.1–BBLE5.3). Fraction BBLE5.2 (523 mg) was purified by HPLC (MeCN/H_2O, isocratic 55%–45%) to give **6** (42.0 mg).

Spectral data

*Lupeol (**1**):* white needle-shaped crystals; ^{1}H-NMR (600 MHz, $CDCl_3$, δ, ppm): 4.69 (1H, d, J=1.8 Hz, H-29a), 4.57 (1H, brs, H-29b), 3.19 (1H, dd, *J* = 4.8, 11.4 Hz, H-3), 1.68 (3H, s, H-30), 1.06 (3H, s, H-26), 0.97 (3H, s, H-23), 0.95 (3H, s, H-27), 0.83 (3H, s, H-25), 0.79 (3H, s, H-28), 0.76 (3H, s, H-24); ^{13}C-NMR (150 MHz, $CDCl_3$): δ_C 151.0 (C-20), 109.3 (C-29), 79.0 (C-3), 55.4 (C-5), 50.5 (C-9), 48.4 (C-18), 48.0 (C-19), 43.0 (C-17), 42.9 (C-14), 40.9 (C-8), 40.0 (C-22), 38.9 (C-4), 38.8 (C-1), 38.1 (C-13), 37.2 (C-10), 35.6 (C-16), 34.3 (C-7), 29.9 (C-21), 28.0 (C-23), 27.5 (C-2), 27.5 (C-15), 25.2 (C-12), 21.0 (C-11), 19.3 (C-30), 18.4 (C-6), 18.0 (C-28), 16.1 (C-25), 16.0 (C-26), 15.4 (C-24), 14.6 (C-27); ESI-MS: m/z 427 $[M+H]^+$.

*Lupenone (**2**):* white powder; ^{1}H-NMR (600 MHz, $CDCl_3$, δ, ppm): 4.69 (1H, d, *J* = 1.0 Hz, H-29a), 4.57 (1H, q, *J* = 1.0 Hz, H-29b), 1.68 (3H, s, H-30), 1.09 (6H, s, H-23 and H-26), 1.04 (3H, s, H-24), 0.97 (3H, s, H-27), 0.95 (3H, s, H-25), 0.80 (3H, s, H-28); ^{13}C-NMR (150 MHz, $CDCl_3$): δ_C 218.1 (C-3), 150.9 (C-20), 109.4 (C-29), 55.0 (C-5), 49.8 (C-9), 48.3 (C-18), 48.0 (C-19), 47.3 (C-4), 43.0 (C-17), 42.9 (C-14), 40.8 (C-8), 40.0 (C-22), 39.6 (C-1), 38.2 (C-13), 36.9 (C-10), 35.5 (C-16), 34.2 (C-2), 33.6 (C-7), 29.9 (C-21), 27.5 (C-15), 26.7 (C-23), 25.2 (C-12), 21.5 (C-11), 21.0 (C-24), 19.7 (C-6), 19.3 (C-30), 18.0 (C-28), 16.0 (C-25), 15.8 (C-26), 14.5 (C-27); ESI-MS: m/z 425 $[M+H]^+$.

*Betulin (**3**):* white powder; ^{1}H-NMR (600 MHz, $CDCl_3$, δ, ppm): 4.68 (1H, brs, H-29a), 4.58 (1H, brs, H-29b), 3.80 (1H, d, *J* = 10.8 Hz, H-28a), 3.34 (1H, d, *J* = 10.8 Hz, H-28b), 3.19 (1H, dd, *J* = 11.4, 4.8 Hz, H-3), 1.68 (3H, s, H-30), 1.03 (3H, s, H-27), 0.98 (3H, s, H-26), 0.97 (3H, s, H-

23), 0.83 (3H, s, H-25), 0.76 (3H, s, H-24); ^{13}C-NMR (150 MHz, $CDCl_3$): δ_C 150.5 (C-20), 109.7 (C-29), 79.0 (C-3), 60.6 (C-28), 55.3 (C-5), 50.5 (C-9), 48.8 (C-18), 47.8 (C-17), 47.8 (C-19), 42.8 (C-14), 41.0 (C-8), 38.9 (C-4), 38.8 (C-1), 38.8 (C-30), 37.4 (C-13), 37.2 (C-10), 34.3 (C-7), 34.0 (C-22), 29.8 (C-21), 29.2 (C-16), 28.0 (C-23), 27.4 (C-2), 27.1 (C-15), 25.3 (C-12), 20.9 (C-11), 18.3 (C-6), 16.1 (C-25), 16.0 (C-26), 15.4 (C-24), 14.8 (C-27); ESI-MS: m/z 443 $[M+H]^+$.
4-Hydroxybenzaldehyde (**4**): pale yellow powder; ^{1}H-NMR (600 MHz, DMSO-d_6, δ, ppm): 9.79 (1H, s, H-7), 7.77 (2H, d, *J* = 8.4 Hz, H-2 and H-6), 6.94 (2H, d, *J* = 8.4 Hz, H-3 and H-5); ^{13}C-NMR (150 MHz, DMSO-d_6): δ_C 190.9 (C-7), 163.3 (C-4), 132.0 (C-2 and C-6), 128.4 (C-1), 115.8 (C-3 and C-5); ESI-MS: m/z 121 $[M-H]^-$.

*β-Sitosterol (**5**):* white powder; ^{1}H-NMR (600 MHz, $CDCl_3$, δ, ppm): 5.35 (1H, m, H-6), 3.53 (1H, m, H-3), 0.99 (3H, s, H-19), 0.93 (3H, d, *J* = 6.6 Hz, H-21), 0.91 (3H, d, *J* = 6.6 Hz, H-26), 0.85 (3H, d, *J* = 7.2 Hz, H-30), 0.83 (3H, d, *J* = 7.2 Hz, H-27), 0.68 (3H, s, H-18); ^{13}C-NMR (150 MHz, $CDCl_3$): δ_C 140.8 (C-5), 121.7 (C-6), 71.8 (C-3), 56.8 (C-14), 56.1 (C-17), 50.2 (C-9), 45.9 (C-24), 42.3 (C-13), 42.2 (C-4), 39.8 (C-12), 37.3 (C-1), 36.5 (C-10), 36.2 (C-20), 34.0 (C-22), 31.9 (C-7), 31.7 (C-2), 29.7 (C-8), 29.2 (C-25), 28.2 (C-16), 26.1 (C-23), 24.3 (C-15), 23.1 (C-28), 21.1 (C-11), 19.8 (C-19), 19.4 (C-26), 19.1 (C-27), 18.8 (C-21), 12.0 (C-29), 11.9 (C-18); ESI-MS: m/z 413 $[M-H]^-$.

*Quercetin (**6**):* yellow powder; ^{1}H-NMR (600 MHz, DMSO-d_6, δ, ppm): 12.47 (1H, brs, 5-OH), 7.67 (1H, d, *J* = 1.8 Hz, H-2′), 7.52 (1H, dd, *J* = 1.8, 8.4 Hz, H-6′), 6.88 (1H, d, *J* = 8.4 Hz, H-5′), 6.40 (1H, d, *J* = 2.4 Hz, H-8), 6.18 (1H, d, *J* = 2.4 Hz, H-6); ^{13}C-NMR (150 MHz, DMSO-d_6): δ_C 175.8 (C-4), 163.9 (C-7), 160.7 (C-5), 156.1 (C-9), 147.7 (C-2), 146.8 (C-4′), 145.0 (C-3′), 135.7 (C-3), 121.9 (C-6′), 119.9 (C-1′), 115.6 (C-5′), 115.0 (C-2′), 103.0 (C-10), 98.1 (C-6), 93.3 (C-8); ESI-MS: m/z 301 $[M-H]^-$.

*Ursolic acid (**7**):* white powder; ^{1}H-NMR (600 MHz, methanol-d_4 and $CDCl_3$, δ, ppm): 5.25 (1H, t, *J* = 3.6 Hz, H-12), 3.19 (1H, dd, *J* = 9.0, 6.6 Hz, H-3), 1.10 (3H, s, H-27), 1.00 (3H, s, H-23), 0.96 (3H, s, H-25), 0.95 (3H, d, *J* = 3.6 Hz, H-30), 0.87 (3H, d, *J* = 6.6 Hz, H-29), 0.83 (3H, s, H-26), 0.78 (3H, s, H-24); ^{13}C-NMR (150 MHz, methanol-d_4 and $CDCl_3$): δ_C 180.5 (C-28), 138.2 (C-13), 125.5 (C-12), 78.7 (C-3), 55.3 (C-5), 52.8 (C-18), 47.8 (C-9), 47.5 (C-17), 42.0 (C-14), 39.4 (C-8), 39.1 (C-19), 38.9 (C-20), 38.7 (C-1), 38.6 (C-4), 36.9 (C-22), 36.8 (C-10), 33.0 (C-7), 30.6 (C-21), 28.0 (C-15), 27.9 (C-23), 26.7 (C-2), 24.2 (C-16), 23.4 (C-11), 23.2 (C-27), 21.0 (C-30), 18.3 (C-6), 16.9 (C-26), 16.8 (C-29), 15.5 (C-24), 15.3 (C-25); ESI-MS: m/z 455 $[M-H]^-$.

*Betulinic acid (**8**):* white powder; ^{1}H-NMR (600 MHz, $CDCl_3$, δ, ppm): 4.74 (1H, s, H-29a), 4.61 (1H, s, H-29b), 3.20 (1H, dd, *J* = 10.8, 4.8 Hz, H-3), 3.00 (1H, td, *J* = 10.8, 4.8 Hz, H-19), 1.70 (3H, s, H-30), 0.98 (3H, s, H-27), 0.97 (3H, s, H-23), 0.94 (3H, s, H-26), 0.83 (3H, s, H-25), 0.76 (3H, s, H-24); ^{13}C-NMR (150 MHz, $CDCl_3$): δ_C 180.4 (C-28), 150.4 (C-20), 109.7 (C-29), 79.1 (C-3), 56.3 (C-17), 55.4 (C-5), 50.6 (C-9), 49.3 (C-18), 46.9 (C-19), 42.5 (C-14), 40.7 (C-8), 38.9 (C-4), 38.8 (C-1), 38.4 (C-13), 37.3 (C-10), 37.1 (C-22), 34.4 (C-7), 32.2 (C-16), 30.6 (C-15), 29.7 (C-21), 28.0 (C-23), 27.4 (C-2), 25.5 (C-12), 20.9 (C-11), 19.4 (C-30), 18.3 (C-6), 16.1 (C-25), 16.1 (C-26), 15.4 (C-24), 14.7 (C-27); ESI-MS: m/z 455 $[M-H]^-$.

Antioxidant activity

The DPPH radical scavenging assay was conducted according to a previously published method [20] with slight adjustments. Samples were prepared in 70% ethanol to test concentrations and combined with a 3 mM DPPH solution in a 1:1 (v/v) ratio. The mixture was kept in the dark for 30 minutes before measuring absorbance at 517 nm using a spectrophotometer. Trolox served as

the positive control, while ionized water was used as the negative control (NC). The percentage of DPPH scavenging activity was calculated using the formula:

$$\text{Radical scavenging activity (\%)} = [(A_{NC} - A_S) / A_{NC}] \times 100 \quad (1)$$

where A_{NC} represents the absorbance of the negative control and A_S denotes the absorbance of the sample. IC_{50} values were determined from the concentration–activity relationship using a nonlinear fitted model in GraphPad Prism (version 8.4.2, GraphPad Software, San Diego, CA, USA). A lower IC_{50} indicates stronger scavenging activity.

The ABTS assay was performed following a reported protocol [21] with minor modifications. $ABTS^{\bullet+}$ radicals were generated by mixing ABTS (2.6 mM) and potassium persulfate (7.4 mM) in a 3:1 ratio and incubating at room temperature for 30 min. The solution was diluted with phosphate-buffered saline (PBS, 0.1 M, pH 7.4) to an absorbance of 0.70 ± 0.02 at 734 nm. Test samples were combined with $ABTS^{\bullet+}$ solution (1:4, v/v) and incubated for 10 min at room temperature, after which absorbance was measured at 734 nm. Trolox and ionized water served as positive and negative controls, respectively. Radical scavenging activity (%) was calculated using Equation (1), and IC_{50} values were determined by nonlinear regression of dose–response curves using GraphPad Prism (v8.4.2, GraphPad Software, San Diego, CA, USA).

α-Amylase inhibitory activity

The α-amylase inhibition assay was conducted following a reported protocol [22] with minor modifications. Enzyme solution (2.5 U/mL), test samples, and acarbose were prepared in PBS (0.1 M, pH 6.9). Reactions contained 100 µL of sample or acarbose mixed with 100 µL of enzyme and incubated for 5 min at room temperature, followed by the addition of 250 µL gelatinized potato starch (0.5%) and 250 µL PBS. After 20 min, the reaction was terminated with 300 µL DNS reagent and heated at 100 °C for 5 min. The mixture was diluted to 1.5 mL with distilled water, and absorbance was recorded at 540 nm. The inhibition was calculated using the following equation:

$$\text{Inhibition (\%)} = [(A_{NC} - A_S)/A_{NC}] \times 100 \quad (2)$$

where A_{NC} and A_S represent the absorbance of the negative control and the sample, respectively. IC_{50} values were obtained by nonlinear regression of sigmoidal dose–response curves using GraphPad Prism (v8.4.2, GraphPad Software, San Diego, CA, USA).

α-Glucosidase inhibitory activity

The α-glucosidase inhibition assay was conducted following a reported protocol [22] with minor modifications. In brief, 20 µL of enzyme (0.1 U/mL) was combined with 20 µL of test sample or acarbose and 140 µL phosphate buffer (0.1 M, pH 6.9), then incubated for 5 min at room temperature. The reaction was initiated with 20 µL p-nitrophenyl-α-D-glucopyranoside (2 mM) and allowed to proceed for 20 min before termination with 100 µL sodium carbonate (0.1 M). Absorbance was recorded at 405 nm. Acarbose served as the positive control, while PBS was used as the negative control. Inhibition (%) was calculated using Equation (2), and IC_{50} values were obtained by nonlinear regression of dose–response curves, consistent with the α-amylase assay.

Molecular docking

The molecular docking study was performed to evaluate the binding affinity and interaction modes of the selected antioxidant compounds isolated from B. bidoupensis leaves toward the Keap1 protein target. The crystal structure of Keap1 (PDB ID: 4L7B) was retrieved from the RCSB Protein Data Bank and prepared by removing water molecules, co-crystallized ligands, and

adding missing hydrogen atoms [23]. The protein structure was subsequently converted to the PDBQT format using AutoDockTools. All ligands were energy-minimized, assigned Gasteiger charges, and saved in PDBQT format prior to docking. Molecular docking simulations were carried out using the AutoDock Vina v1.2.3 program, employing an exhaustiveness value sufficient to ensure thorough conformational sampling [24, 25] . The grid box was centered on the Kelch domain binding pocket, covering all key residues involved in Keap1–Nrf2 recognition. For each ligand, the best-ranked pose was selected based on the Vina binding affinity score and further analyzed for hydrogen bonding and hydrophobic interactions using Discovery Studio Visualizer software. This approach enabled reliable prediction of ligand–Keap1 interactions relevant to antioxidant activity.

RESULTS AND DISCUSSION

Structural data of isolated compounds

The ^{1}H-NMR spectrum of **1** exhibited seven methyl signals at δ_H 1.68 (3H, s, H-30), 1.06 (3H, s, H-26), 0.97 (3H, s, H-23), 0.95 (3H, s, H-27), 0.83 (3H, s, H-25), 0.79 (3H, s, H-28), and 0.76 (3H, s, H-24), while the ^{13}C-NMR spectrum showed 30 carbon resonances, suggesting that compound **1** possesses a triterpenoid skeleton. The ^{1}H-NMR spectrum also displayed a pair of signals at δ_H 4.69 (1H, d, J = 1.8 Hz, H-29a) and 4.57 (1H, brs, H-29b), corresponding to a terminal methylene group, which is indicative of a lupane-type triterpenoid. This hypothesis is further supported by the ^{13}C-NMR spectroscopic data, which include signals at δ_C 151.0 (C-20) and 109.3 (C-29), attributable to a terminal double bond, and a signal at δ_H 79.0 assignable to an oxygenated carbon, typically located at C-3 of the lupane triterpenoid. The HMBC correlations of H-29 with C-19, C-20, and C-30 establish the position of the terminal methylene group, a characteristic feature of the lupane skeleton. Comparison of the NMR data of **1** with those reported in the literature confirms that **1** is lupeol [26-29].

The ^{1}H and ^{13}C-NMR spectra of **2** share similar patterns with those of **1**, including seven methyl groups at δ_H 1.68 (3H, s, H-30), 1.09 (6H, s, H-23 and H-26), 1.04 (3H, s, H-24), 0.97 (3H, s, H-27), 0.95 (3H, s, H-25), and 0.80 (3H, s, H-28), a terminal double bond at δ_H 4.69 (1H, d, J = 1.0 Hz, H-29a) and 4.57 (1H, q, J = 1.0 Hz, H-29b); with a total of 30 carbon signals, suggesting that **2** also possesses a lupane-type skeleton. The ^{13}C-NMR spectrum showed a ketonic carbonyl signal at δ_C 218.1 and the absence of an oxygenated carbon signal at C-3, which is typically observed around δ_C 70–80, indicating the presence of a ketone at C-3. HMBC correlations of H-29 with C-19, C-20, and C-30 confirm the position of the terminal methylene group, a characteristic feature of the lupane skeleton. The position of the carbonyl group is further established by HMBC correlations from H-1, H-2, H-23, and H-24 to C-3. Comparison of the NMR data of **2** with those reported in the literature confirms that **2** is lupenone [26, 28].

The ^{1}H and ^{13}C-NMR spectra of **3** was also found to possess the similar patterns with those of **1** and **2**, such as the methyl groups at δ_H 1.68 (3H, s, H-30), 1.03 (3H, s, H-27), 0.98 (3H, s, H-26), 0.97 (3H, s, H-23), 0.83 (3H, s, H-25), and 0.76 (3H, s, H-24); a terminal double bond at δ_H 4.68 (1H, brs, H-29a) and 4.58 (1H, brs, H-29b); with 30 carbon signals, indicating that **3** also possesses a lupane-type skeleton. However, the number of methyl groups was only six, indicating that one methyl group was oxidized to a different group. The ^{1}H-NMR spectrum showed oxygenated proton signals at δ_H 3.80 (1H, d, J = 10.8 Hz, H-28a) and 3.34 (1H, d, J = 10.8 Hz, H-28b), suggesting that the methyl group at C-28 (δ_C 60.6) has been transformed into an oxymethylene group. HMBC correlations of H-29 with C-19, C-20, and C-30 confirm the position of the terminal methylene group, an indicative feature of the lupane triterpenoid. The position of the oxymethylene group is established by HMBC correlations from H-28 to C-16, C-17, and C-22. Comparison of the NMR data of **3** with those reported in the literature confirms that **3** is betulin [26, 30].

The ^{1}H-NMR spectrum of **4** showed two signals at δ_H 7.77 (2H, d, J = 8.4 Hz, H-2 and H-6) and 6.94 (2H, d, J = 8.4 Hz, H-3 and H-5), corresponding to an A_2B_2 spin system, along with a singlet at δ_H 9.79 (1H, s, H-7). In combination with the signal at δ_C 190.9 (C-7) in the ^{13}C-NMR spectrum and HSQC correlation, these data indicate the presence of an aldehyde functional group in the molecule. Comparison of the NMR data of **4** with those reported in the literature suggests that **4** is 4-hydroxybenzaldehyde [31].

The ^{1}H-NMR spectrum of **5** showed the presence of multiple characteristic signals at δ_H 5.35 (m, 1H), 1.03 (s, 3H), 0.91 (d, 3H, J = 6.2 Hz), 0.83 (t, 3H, J = 7.1 Hz), 0.82 (d, 3H, J = 6.6 Hz), 0.80 (d, 3H, J = 6.6 Hz), and 0.71 (s, 3H). In addition, the ^{13}C-NMR spectrum displays 29 carbon signals, indicating that **5** is a typical phytosterol containing one double bond, an isopropyl group, and an ethyl group in its structure. Comparison of the NMR data of **5** with those reported in the literature indicates that **5** is β-sitosterol [28, 32]. This compound is a very common phytosterol and is present in the majority of plant species.

The ^{1}H-NMR spectrum of **6** exhibited characteristic resonances of a flavonol skeleton, with signals at δ_H 7.67 (1H, d, J = 1.8 Hz, H-2′), 7.52 (1H, dd, J = 1.8, 8.4 Hz, H-6′), and 6.88 (1H, d, J = 8.4 Hz, H-5′), corresponding to an ABX spin system on B-ring, and two signals at δ_H 6.40 (1H, d, J = 2.4 Hz, H-8) and 6.18 (1H, d, J = 2.4 Hz, H-6) assignable to A-ring. A downfield proton signal at δ_H 12.47 (1H, brs, 5-OH) indicates the presence of an intramolecular hydrogen bond between the carbonyl group and the hydroxyl group at C-5. The ^{13}C-NMR spectrum displayed 15 carbon resonances all located in the downfield region, specifically aromatic and carbonyl carbons, further supporting the presence of a flavonol skeleton. HMBC correlations provide additional key structural information, including correlations between H-2′ and C-2, and between H-6 and H-8 with C-10. Comparison of the NMR data of **6** with those reported in the literature confirms that **6** is quercetin [33].

The ^{1}H-NMR spectrum of **7** showed seven methyl signals at δ_H 1.10 (3H, s, H-27), 1.00 (3H, s, H-23), 0.96 (3H, s, H-25), 0.95 (3H, d, J = 3.6 Hz, H-30), 0.87 (3H, d, J = 6.6 Hz, H-29), 0.83 (3H, s, H-26), and 0.78 (3H, s, H-24), while the ^{13}C-NMR spectrum exhibited 30 carbon resonances, suggesting that compound **7** possesses a triterpenoid skeleton. The ^{13}C-NMR data further revealed the presence of a carboxylic acid carbon at δ_C 180.5 (C-28). In combination with the two methyl doublets at δ_H 0.87 (H-29) and 0.95 (H-30), these findings support the hypothesis that **7** has an ursane-type triterpenoid. Key HMBC correlations between H-29/H-30 and C-20, between H-16/H-18/H-22 and C-28 support the abovementioned deduction. Comparison of the NMR data of **7** with those reported in the literature confirms that **7** is ursolic acid [34].

The ^{1}H and ^{13}C-NMR spectra of **8** also showed similarities with those of **3** including six methyl groups at δ_H 1.70 (3H, s, H-30), 0.98 (3H, s, H-27), 0.97 (3H, s, H-23), 0.94 (3H, s, H-26), 0.83 (3H, s, H-25), and 0.76 (3H, s, H-24), a terminal double bond at δ_H 4.74 (1H, s, H-29a) and 4.61 (1H, s, H-29b); and a total of 30 carbon signals, indicating that **8** is also a lupane-type triterpenoid. The ^{13}C-NMR spectrum shows a carboxylic carbon resonance at δ_C 180.4 (C-28), suggesting that one methyl group has been oxidized to a carboxylic acid functional group. The position of the carboxylic acid group is established by HMBC correlations between H-16/H-22 and C-28. Comparison of the NMR data of **8** with those reported in the literature confirms that **8** is betulinic acid [35].

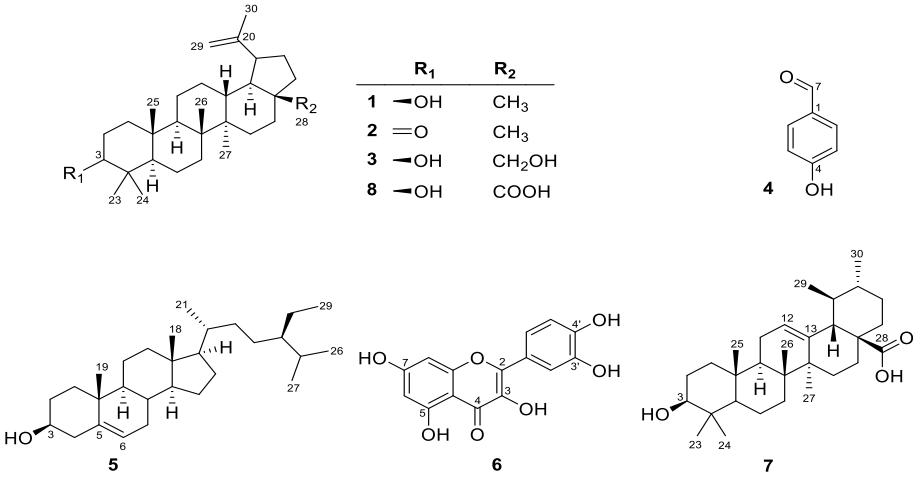

Figure 2. Structures of isolated compounds (**1**-**8**) from *B. bidoupensis*.

In the present work, eight compounds were isolated from the leaves of *B. bidoupensis*. These belong to several classes, including five triterpenoids (**1**–**3**, **7**, and **8**), a phenolic (**4**), a steroid (**5**), and a flavonoid (**6**). Their structures (Figure 2) were confirmed by analyzing their spectroscopic data and comparing them with established literature values. This is the first report of the isolation of these compounds from *B. bidoupensis.*

In vitro antioxidant activity of the chemical constituents

Among the eight compounds isolated from *B. bidoupensis*, only quercetin (**6**) exhibited strong antioxidant activity, with IC_{50} values of 15.88 ± 0.66 μM (DPPH) and 6.82 ± 0.17 μM (ABTS). These values were markedly lower than those of Trolox (IC_{50} = 157.46 ± 4.87 μM for DPPH and 40.39 ± 1.96 μM for ABTS), indicating superior radical-scavenging capacity. In contrast, other compounds showed no detectable activity in the DPPH assay, whereas compounds **4** and **8** exhibited weak activity in the ABTS assay (IC_{50} = 15877.83 ± 587.05 μM and 4497.3 ± 20.44 μM, respectively) (Table 1). These findings suggest that the antioxidant potential of *B. bidoupensis* is primarily attributable to flavonoid constituents, consistent with previous reports on quercetin's strong free radical-neutralizing properties.

Table 1. Antioxidant activity of constituents of *B. bidoupensis.*

Compounds	IC_{50} (μM)	
	DPPH	ABTS
Lupeol (**1**)	n.d.	n.d.
Lupenone (**2**)	n.d.	n.d.
Betulin (**3**)	n.d.	n.d.
4-Hydroxybenzaldehyde (**4**)	n.d.	15877.83 ± 587.05^{C}
β-Sitosterol (**5**)	n.d.	n.d.
Quercetin (**6**)	15.88 ± 0.66^{A}	6.82 ± 0.17^{A}
Ursolic acid (**7**)	n.d.	n.d.
Betulinic acid (**8**)	n.d.	4497.30 ± 20.44^{B}
Trolox	157.46 ± 4.87^{B}	40.39 ± 1.96^{A}

Values are presented as mean ± SD (n = 3). Superscript letters indicate statistically significant differences within each column ($p < 0.05$). n.d.: not detected.

Compared with other *Beilschmiedia* species, the activities of bark oils from *B. maingayi* and *B. penangiana* were positively correlated to high total phenolic content (TPC > 280 mg GA/g) [36]. Similarly, methanolic bark extracts of *B. insignis*, which are rich in polyphenolic compounds, exhibited the strongest antioxidant effects in both DPPH and FRAP assays [37]. These results confirm that polar phenolic compounds—particularly quercetin—are the primary contributors to antioxidant activity in *B. bidoupensis*. The remarkably low IC_{50} values observed for compound **6**, when compared to Trolox and other *Beilschmiedia* extracts highlight its superior radical-scavenging capacity. In contrast, the lack of activity among triterpenoids and sterols supports previous evidence that non-phenolic constituents have minimal antioxidant roles, despite their relevance in other biological pathways.

In vitro α-amylase and α-glucosidase inhibitory activities of the chemical constituents

Quercetin (**6**) exhibited the strongest α-glucosidase inhibitory activity among the isolated compounds, with an IC_{50} value of 31.1 ± 3.14 μM (Table 2). Ursolic acid (**7**) also showed notable inhibitory activity (IC_{50} = 458.07 ± 52.59 μM), whereas betulinic acid (**8**), 4-hydroxybenzaldehyde (**4**), and betulin (**3**) displayed weaker activities, with IC_{50} values of 1493.79 ± 343.54, 3034.47 ± 531.61, and 4560.65 ± 1999.37 μM, respectively. Based on the statistical analysis, quercetin (**6**), ursolic acid (**7**), betulinic acid (**8**), and the positive control acarbose (833.69 ± 89.89 μM) were not significantly different from one another ($p > 0.05$), whereas 4-hydroxybenzaldehyde (**4**) and betulin (**3**) exhibited significantly weaker inhibitory effects. In contrast, all tested compounds showed no detectable activity against *α*-amylase under the experimental conditions (n.d.). These results identify quercetin as the principal α-glucosidase inhibitory constituent of *B. bidoupensis*. The selective inhibition of α-glucosidase, together with the absence of α-amylase inhibition, suggests a targeted mechanism that may help moderate postprandial glucose absorption while potentially reducing the gastrointestinal side effects commonly associated with non-selective carbohydrate-hydrolyzing enzyme inhibitors such as acarbose.

Table 2. *α*-Amylase and *α*-glucosidase inhibitory activities of constituents of *B. bidoupensis.*

Compounds	IC_{50} (μM)	
	α-amylase	*α*-glucosidase
Lupeol (**1**)	n.d.	n.d.
Lupenone (**2**)	n.d.	n.d.
Betulin (**3**)	n.d.	4560.65 ± 1999.37^{C}
4-Hydroxybenzaldehyde (**4**)	n.d.	3034.47 ± 531.61^{B}
β-Sitosterol (**5**)	n.d.	n.d.
Quercetin (**6**)	n.d.	31.1 ± 3.14^{A}
Ursolic acid (**7**)	n.d.	458.07 ± 52.59^{A}
Betulinic acid (**8**)	n.d.	1493.79 ± 343.54^{A}
Acarbose	234.36 ± 52.82	833.69 ± 89.89^{A}

Values are presented as mean ± SD (n = 3). Superscript letters indicate statistically significant differences within each column ($p < 0.05$). n.d.: not detected.

Compared with other *Beilschmiedia* species, the inhibitory potency of the isolated compounds particularly for quercetin (**6**) from *B. bidoupensis* is noteworthy. Methanolic bark extracts of *B. insignis* have been reported to demonstrate exceptionally strong inhibition of both *α*-amylase and *α*-glucosidase [37], our findings show that quercetin (**6**) possesses an even more potent and

selective *α*-glucosidase inhibition. This selectivity mirrors dietary studies on wine and tea extracts, which strongly inhibit *α*-glucosidase but only mildly affect *α*-amylase, thereby slowing glucose absorption while minimizing gastrointestinal discomfort [22]. Such selectivity is considered advantageous over synthetic inhibitors like acarbose, which strongly block both enzymes and often cause adverse effects due to undigested starch fermentation. Collectively, these findings indicate that phenolic constituents, particularly quercetin, are the primary contributors to the α-glucosidase inhibitory activity of *B. bidoupensis* and highlight their potential as selective anti-hyperglycemic agents.

Molecular docking

The docking protocol was first validated through a re-docking experiment using the reference ligand 1VV co-crystallized in Keap1 (PDB ID: 4L7B). The re-docked pose reproduced the experimental binding orientation with an RMSD of 1.724 Å (Figure 3), which is below the widely accepted threshold of 2.0 Å, confirming the reliability and accuracy of the docking parameters. Subsequently, antioxidant compounds were further investigated for their binding interactions with the target protein Keap1 (Kelch-like ECH-associated protein 1), the key negative regulator of the Nrf2 antioxidant pathway whose Kelch domain binds and promotes Nrf2 degradation. The results are presented in Table 3 and Figure 4. Among the tested antioxidant constituents from *B. bidoupensis*, quercetin exhibited a strong binding affinity (−8.564 kcal/mol), approaching that of the reference ligand (−10.15 kcal/mol). Quercetin formed multiple stabilizing hydrogen bonds with Asn414, Ser363, and Ser383, along with aromatic interactions including π–π stacking and π–π T-shaped contacts with Tyr334 and Tyr572. Additional π–sigma and π–alkyl interactions involving Tyr572, Arg415, and Ala556. Notably, both the interaction pattern of quercetin closely mirrors those of the reference ligand, highlighting its potential as a Keap1 inhibitor. Betulinic acid also demonstrated a favorable binding score (−8.427 kcal/mol), supported predominantly by hydrophobic interactions such as π–sigma (Tyr525) and π–alkyl/alkyl contacts with amino acid residues Ala556, Arg415, Tyr572, and Tyr334. These interactions suggest that betulinic acid is well accommodated within the hydrophobic core of the Keap1 Kelch domain. In contrast, 4-hydroxybenzaldehyde displayed a weaker affinity (−5.775 kcal/mol), forming only a limited number of stabilizing contacts, including a hydrogen bond with Ser602, π–sigma and donor–π interactions with Tyr572, and a π–π stacked interaction with Tyr334. The relatively small molecular size and fewer functional groups available for interaction likely contributed to its reduced binding strength. The docking results highlight quercetin and betulinic acid as the most promising inhibitors of Keap1 among the evaluated phytochemicals, exhibiting interaction patterns comparable to the reference ligand and favorable predicted binding energies. These findings are in line with previous mechanistic studies showing that quercetin can activate the Nrf2 pathway by enhancing ARE-binding activity, stabilizing Nrf2, and reducing Keap1 protein levels through posttranslational modifications rather than proteasomal degradation [38]. Similarly, betulinic acid has been shown to mitigate oxidative stress via Nrf2/Keap1 signaling, improving cellular antioxidant capacity and resilience to ROS [39]. Additionally, quercetin (**6**) and related flavonoids have been extensively investigated as inhibitors of *α*-glucosidase, showing good agreement between in silico docking and experimental inhibitory activity, along with well-characterized interaction mechanisms involving hydrophobic forces and conformational changes [40, 41].

Table 3. Binding affinities and key interactions of selected compounds with Keap1 protein.

Compounds	Binding affinity (kcal/mol)	Interaction types	Involved Amino acid residues
Quercetin (**6**)	-8.564	Hydrogen bond	Asn414, Ser363, Ser383
		Unfavorable Donor-Donor	Asn387

		Pi-Sigma	Tyr572
		Pi-Pi-Stacked, Pi-Pi T-shaped	Tyr334, Tyr572
		Pi- Alkyl	Arg415, Ala556
Betulinic acid (**8**)	-8.427	Pi-Sigma	Tyr525
		Pi- Alkyl, Alkyl	Ala556, Arg415, Tyr572, Tyr334
4-hydroxybenzaldehyde (**4**)	-5.775	Hydrogen bond	Ser602
		Pi- Donor Hydrogen bond	Tyr572
		Pi-Sigma	Tyr572
		Pi-Pi-Stacked	Tyr334
1VV (ref)	-10.15	Hydrogen bond	Arg415, Ser602, Asn414
		Pi-Sigma	Ala556
		Pi- Alkyl, Alkyl	Ala556, Tyr334, Arg415
		Pi-pi stacked	Tyr572

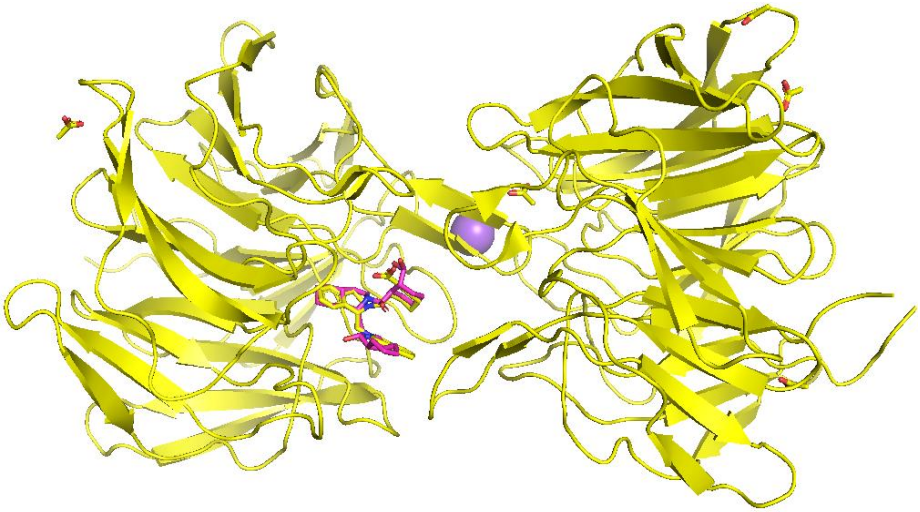

Figure 3. Superimposition of the crystallographic and re-docked poses of 1VV in the Keap1 binding pocket, showing an RMSD of 1.724 Å, validating the docking protocol.

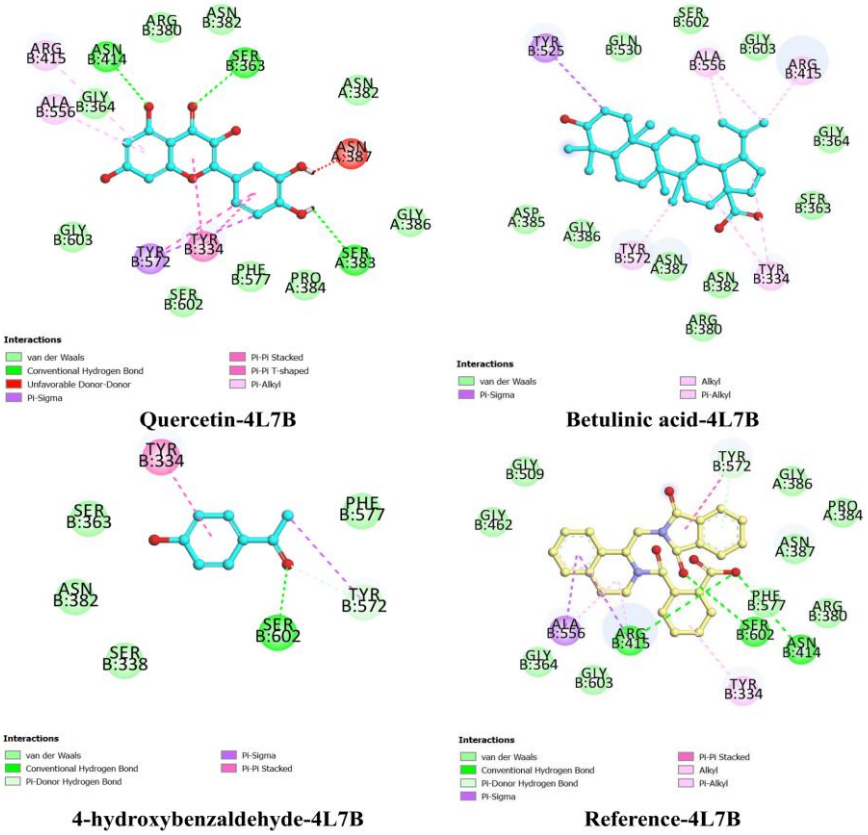

Figure 4. 2D interaction maps of selected compounds in the active-site pocket of Keap1.

CONCLUSIONS

In conclusion, the present work confirms that *B. bidoupensis* leaves are a rich source of diverse secondary metabolites, including triterpenoids, steroids, and phenolics. Quercetin (**6**) emerged as the most potent constituent, exhibiting both superior antioxidant capacity and the strongest *α*-glucosidase inhibitory activity. Additionally, ursolic acid (**7**) and 4-hydroxybenzaldehyde (**4**) showed promising selective *α*-glucosidase inhibitory potential. The isolation, biological evaluation, and molecular docking studies collectively support the potential of *B. bidoupensis* constituents as natural agents for developing novel antioxidants and anti-diabetic lead compounds. Future studies should focus on the *in vivo* anti-diabetic and antioxidant efficacy of the isolated compounds and explore the mechanisms of selective enzyme inhibition in greater detail. Further research could also involve structure-activity relationship (SAR) studies to optimize the potency and selectivity of these natural constituents.

ACKNOWLEDGEMENT

The authors are grateful to the Vietnam Ministry of Education and Training for the financial support provided [grant number B2025-TDV-02].

Ethical approval: The conducted research is not related to either human or animal use.

Data availability statement: The data sets generated and/or analyzed during the current study are available from the corresponding author upon reasonable request.

Conflicts of interest: All authors declare that there are no conflicts of interest.

REFERENCES

1. Nishida, S. Revision of *Beilschmiedia* (Lauraceae) in the neotropics. *Ann. Missouri Bot. Gard.* **1999**, 86, 657-701.
2. Ndjakou, L.B.; Chouna, J.R.; Nkeng-Efouet, P.A.; Sewald, N. Endiandric acid derivatives and other constituents of plants from the genera *Beilschmiedia* and *Endiandra* (Lauraceae). *Biomolecules* **2015**, 5, 910-942.
3. Khanal, L.N.; Sharma, K.R.; Pokharel, Y.R.; Kalauni, S.K. Phytochemical analysis and *in vitro* antioxidant and antibacterial activity of different solvent extracts of *Beilschmiedia roxburghiana* nees stem barks. *Sci. World J.* **2022**, 1, 6717012.
4. Salleh, W.M.N.H.W.; Ahmad, F.; Yen, K.H. Chemical compositions and biological activities of the essential oils of *Beilschmiedia madang* Blume (Lauraceae). *Arch. Pharmacal Res.* **2015**, 38, 485-493.
5. Lenta, B.N.; Tantangmo, F.; Devkota, K.P.; Wansi, J.D.; Chouna, J.R.; Soh, R.C.F.; Neumann, B.; Stammler, H.G.; Tsamo, E.; Sewald, N. Bioactive constituents of the stem bark of *Beilschmiedia zenkeri*. *J. Nat. Prod.* **2009**, 72, 2130-2134.
6. Chouna, J.R.; Nkeng-Efouet, P.A.; Lenta, B.N.; Wansi, J.D.; Kimbu, S.F.; Sewald, N. Endiandric acid derivatives from the stem bark of *Beilschmiedia anacardioides*. *Phytochem. Lett.* **2010**, 3, 13-16.
7. Talontsi, F.M.; Lamshöft, M.; Bauer, J.O.; Razakarivony, A.A.; Andriamihaja, B.; Strohmann, C.; Spiteller, M. Antibacterial and antiplasmodial constituents of *Beilschmiedia cryptocaryoides*. *J. Nat. Prod.* **2013**, 76, 97-102.
8. Setzer, W.N.; Haber, W.A. Leaf essential oil composition of five species of *Beilschmiedia* from Monteverde, Costa Rica. *Nat. Prod. Commun.* **2007**, 2, 1934578X0700200116.
9. Chen, J.J.; Chou, E.T.; Peng, C.F.; Chen, I.S.; Yang, S.Z.; Huang, H.Y. Novel epoxyfuranoid lignans and antitubercular constituents from the leaves of *Beilschmiedia tsangii*. *Planta Med.* **2007**, 73, 567-571.
10. Chouna, J.R.; Nkeng-Efouet, P.A.; Lenta, B.N.; Devkota, K.P.; Neumann, B.; Stammler, H.G.; Kimbu, S.F.; Sewald, N. Antibacterial endiandric acid derivatives from *Beilschmiedia anacardioides*. *Phytochemistry* **2009**, 70, 684-688.
11. Mollataghi, A.; Coudiere, E.; Hadi, A.H.A.; Mukhtar, M.R.; Awang, K.; Litaudon, M.; Ata, A. Anti-acetylcholinesterase, anti-α-glucosidase, anti-leishmanial and anti-fungal activities of chemical constituents of *Beilschmiedia* species. *Fitoterapia* **2012**, 83, 298-302.
12. Salleh, W.M.N.H.W.; Nafiah, M.A.; Jauri, M.H.; Khamis, S. Chemical constituents and acetylcholinesterase inhibitory activity of *Beilschmiedia insignis* Gamble. *Bull. Chem. Soc. Ethiop.* **2021**, 35, 685-691.
13. Huang, Y.T.; Chang, H.S.; Wang, G.J.; Lin, C.H.; Chen, I.S. Secondary metabolites from the roots of *Beilschmiedia tsangii* and their anti-inflammatory activities. *Int. J. Mol. Sci.* **2012**, 13, 16430-16443.
14. Lin, C.T.; Chu, F.H.; Tseng, Y.H.; Tsai, J.B.; Chang, S.T.; Wang, S.Y. Bioactivity investigation of Lauraceae trees grown in Taiwan. *Pharm. Biol.* **2007**, 45, 638-644.
15. Komada, N.; Tagane, S.; Matsuo, A.; Ngoc, N.V.; Binh, H.T.; Nagahama, A.; Cuong, T.Q.; Yahara, T. *Beilschmiedia bidoupensis* (Lauraceae), a new species from Bidoup-Nui Ba National Park, southern highland of Vietnam. *Phytotaxa* **2022**, 559, 285-292.

16. Tran, T.H.; Ha, N.X.; Ba, C.C.; Nguyen, V.T.; Thu, N.T.; Giang, L.D.; Le, C.T. Chemical constituents of the trunk bark of *Pyrularia edulis* (Cervantesiaceae) and their acetylcholinesterase inhibitory activity assessed through *in vitro* and *in silico* approaches. *J. Biol. Act. Prod. Nat.* **2025**, 15, 344-352.
17. Van, S.V.; Tuan, N.H.; Giang, L.D.; Tran, T.H.; Thuan, V.T.; An, N.T.G.; Nguyen, X.H.; Chi, T.L.; Chanh, M.N.; Nguyen, K.D. Antioxidant activities and chemical composition of rhizome essential oil from *Zingiber plicatum* Škorničk. & QB Nguyen from Vietnam. *J. Essent. Oil-Bear. Plants* **2024**, 27, 1121-1129.
18. Hieu, T.T.; Giang, L.D.; Thuan, V.T.; Trung, V.H.; Hieu, N.N.; Duc, N.D.; Truong, Q.C.; Duc, D.X. Chemical composition of essential oils extracted from the leaves and rhizomes of *Alpinia hongiaoensis* Tagane.(Zingiberaceae) growing wild in Vietnam. *J. Essent. Oil-Bear. Plants* **2023**, 26, 396-402.
19. Hieu, T.T.; Purnomo, K.A.; Yu, S.Y.; Yang, Z.J.; Hu, H.C.; Hwang, T.L.; Nguyen, N.T.; Le, N.T.; Dau, X.D.; Le, D.Q.; Anders, B.; Tran, D.T.; Chang, F.R. Anti-inflammatory and Antiphytopathogenic Fungal Activity of 2, 3-seco-Tirucallane Triterpenoids Meliadubins A and B from *Melia dubia* Cav. Barks with ChemGPS-NP and *In Silico* Prediction. *ACS Omega* **2023**, 8, 37116-37127.
20. Khoa, D.N.; Chanh, M.N.; Duy, A.L.; Hung, T.H.; Mai, T.T.; Anh, T.N.T.; Trang, H.D.N.; Danh, C.V.; Lien, T.T.N. The mixture of *Ganoderma lucidum* and *Cordyceps militaris*: Chemical composition and protective effect against oxidative stress. *J. Agric. Food Res.* **2024**, 15, 101045.
21. Nguyen, H.T.; Tran, T.H.; Giang, L.D.; Triet, N.T.; Tran, V.C.; Vu, C.D.; Anh, V.N.; Nhi, N.T.To.; Khoa, V.A.N.; Khoa, D.N. *Alpinia nelumboides* Nob. Tanaka, TTK Van & V. Hoang: phytochemical analysis and antioxidant activities of pseudo-stem and rhizome essential oils. *Nat. Prod. Res.* **2025**, 39, 127-134.
22. Kwon, Y.I.; Apostolidis, E.; Shetty, K. Inhibitory potential of wine and tea against α-amylase and α-glucosidase for management of hyperglycemia linked to type 2 diabetes. *J. Food Biochem.* 2008, 32, 15-31.
23. Jnoff, E.; Albrecht, C.; Barker, J.J.; Barker, O.; Beaumont, E.; Bromidge, S.; Frederick, B.; Mark, B.; Christian, B.; Tom, C.; Vincent, C.; Graham, D.; Stephanie, D.; Tara, F.; Christophe, G.; Emilie, J.; Jason, K.; Rosemary, M.; Innocent, M.; Richard, P.; Zara, A.S.; Myron, A.S.; Christopher, C.S.; Courade, J.P. Binding mode and structure–activity relationships around direct inhibitors of the Nrf2–Keap1 complex. *ChemMedChem* **2014**, 9, 699-705.
24. Eberhardt, J.; Santos, M.D.; Tillack, A.F.; Forli, S. AutoDock Vina 1.2. 0: new docking methods, expanded force field, and python bindings. *J. Chem. Inf. Model.* **2021**, 61, 3891-3898.
25. Trott, O.; Olson, A.J. AutoDock Vina: improving the speed and accuracy of docking with a new scoring function, efficient optimization, and multithreading. *J. Comput. Chem.* **2010**, 31, 455-461.
26. Tran, C.K.; Nguyen, T.M.H.; Doan, T.M.H.; Nguyen, V.H. Study on the chemical constituents of the roots of *Pseuderanthemum palatiferum* (Nees) Radlk. (Acanthaceae) (Vietnamese). *Vietnam J. Sci. Technol.* **2007**, 45, 309-314.
27. Wan Mohd, N.H.W.S.; Shakri, N.M.; Nafiah, M.A.; Ghani, N.A.; Rasol, N.E.; Rezali, N.S.; Jauri, M.H. Chemical constituents of the leaves of *Actinodaphne pruinosa*. *Bull. Chem. Soc. Ethiop.* **2022**, 36, 963-969.
28. Salleh, W.M.N.H.W.; Nafiah, M.A.; Tawang, A. Chemical constituents and acetylcholinesterase inhibitory activity of *Piper abbreviatum* Opiz. *Bull. Chem. Soc. Ethiop.* **2020**, 34, 625-632.

29. Alharbi, N.A.; Mohamed, G.A.; Abdallah, H.M.; Alfaifi, M.Y.; Elbehairi, S.E.I.; Ibrahim, S.R. Cytotoxic metabolites from the aerial part of *Onopordum heteracanthum* growing in Saudi Arabia. *Bull. Chem. Soc. Ethiop.* **2026**, 40, 2069-2080.
30. Tijjani, A.; Ndukwe, I.G.; Ayo, R.G. Isolation and characterization of lup-20 (29)-ene-3, 28-diol (Betulin) from the stem-bark of *Adenium obesum* (Apocynaceae). *Trop. J. Pharm. Res.* **2012**, 11, 259-262.
31. Wang, G.B.; Wang, Y.J.; Kan, J.L.; Xie, K.H.; Xu, H.P.; Zhao, F.; Wang, M.C.; Geng, Y.; Dong, Y.B. Construction of covalent organic frameworks via a visible-light-activated photocatalytic multicomponent reaction. *J. Am. Chem. Soc.* **2023**, 145, 4951-4956.
32. Quan, P.M.; Van, T.T.H.; Phuong, D.L.; Ich, C.T.; Long, P.Q., Minh, P.T.H. Study on the chemical constituents of *Urena lobata* growing in Viet Nam. *Vietnam J. Sci. Technol.* **2019**, 57, 162-169.
33. Van, N.T.H.; Bach, P.C.; Ich, C.T.; Phuong, D.L.; Thanh, L.T.; Toan, T.Q.; Long, P.Q. Flavonoids isolated from the flowers of *Camellia chrysantha*. *Vietnam J. Sci. Technol.* **2019**, 57, 287-293.
34. Seebacher, W.; Simic, N.; Weis, R.; Saf, R.; Kunert, O. Complete assignments of ^{1}H and ^{13}C NMR resonances of oleanolic acid, 18α-oleanolic acid, ursolic acid and their 11-oxo derivatives. *Magn. Reson. Chem.* **2003**, 41, 636-638.
35. Kim, J.H.; Byun, J. C.; Bandi, A.K.R.; Hyun, C.G.; Lee, N.H. Compounds with elastase inhibition and free radical scavenging activities from Callistemon lanceolatus. *J. Med. Plants Res.* **2009**, 3, 914-920.
36. Salleh, W.M.N.H.W.; Ahmad, F.; Khong, H.Y.; Mohamed, Z.R. Comparative study of the essential oils of three *Beilschmiedia* species and their biological activities. *Int. J. Food Sci. Technol.* **2016**, 51, 240-249.
37. Tay, Y.N.; Bakar, M.H.A.; Azmi, M.N.; Saad, N.A.; Awang, K.; Litaudon, M.; Kassim, M.A. Inhibition of carbohydrate hydrolysing enzymes, antioxidant activity and polyphenolic content of *Beilschmiedia* species extracts. *IOP Conf. Ser.: Mater. Sci. Eng.* **2020**, 716, 012007.
38. Tanigawa, S.; Fujii, M.; Hou, D.X. Action of Nrf2 and Keap1 in ARE-mediated NQO1 expression by quercetin. *Free Radic. Biol. Med.* **2007**, 42, 1690-1703.
39. Kim, M.J.; Kang, H.G.; Jeon, S.B.; Yun, J.H.; Jeong, P.S.; Sim, B.W.; Kim, S.U.; Cho, S.K.; Song, B.S. The antioxidant betulinic acid enhances porcine oocyte maturation through Nrf2/Keap1 signaling pathway modulation. *Plos One* **2024**, 19, e0311819.
40. Qi, Y.J.; Zhao, Y.M.; Lu, H.N.; Wang, X.E.; Jin, N.Z. Exploring molecular flexibility and the interactions of Quercetin derivatives in the active site of α-glucosidase using molecular docking and charge density analysis. *Comput. Theor. Chem.* **2016**, 1094, 55-68.
41. Zhu, J.; Zhang, B.; Tan, C.; Huang, Q. α-Glucosidase inhibitors: consistency of *in silico* docking data with *in vitro* inhibitory data and inhibitory effect prediction of quercetin derivatives. *Food Funct.* **2019**, 10, 6312-6321.